

Supplementary Information

Graphene-Metal Composite Sensors with Near-Zero Temperature Coefficient of Resistance

Brandon C. Marin, Samuel E. Root, Armando D. Urbina, Eden Aklile, Rachel Miller, Aliaksandr V. Zaretski, Darren J. Lipomi*

Department of NanoEngineering, University of California, San Diego
9500 Gilman Drive, Mail Code 0448, La Jolla, CA 92093-0448

*Author to whom correspondence should be addressed: dlipomi@eng.ucsd.edu

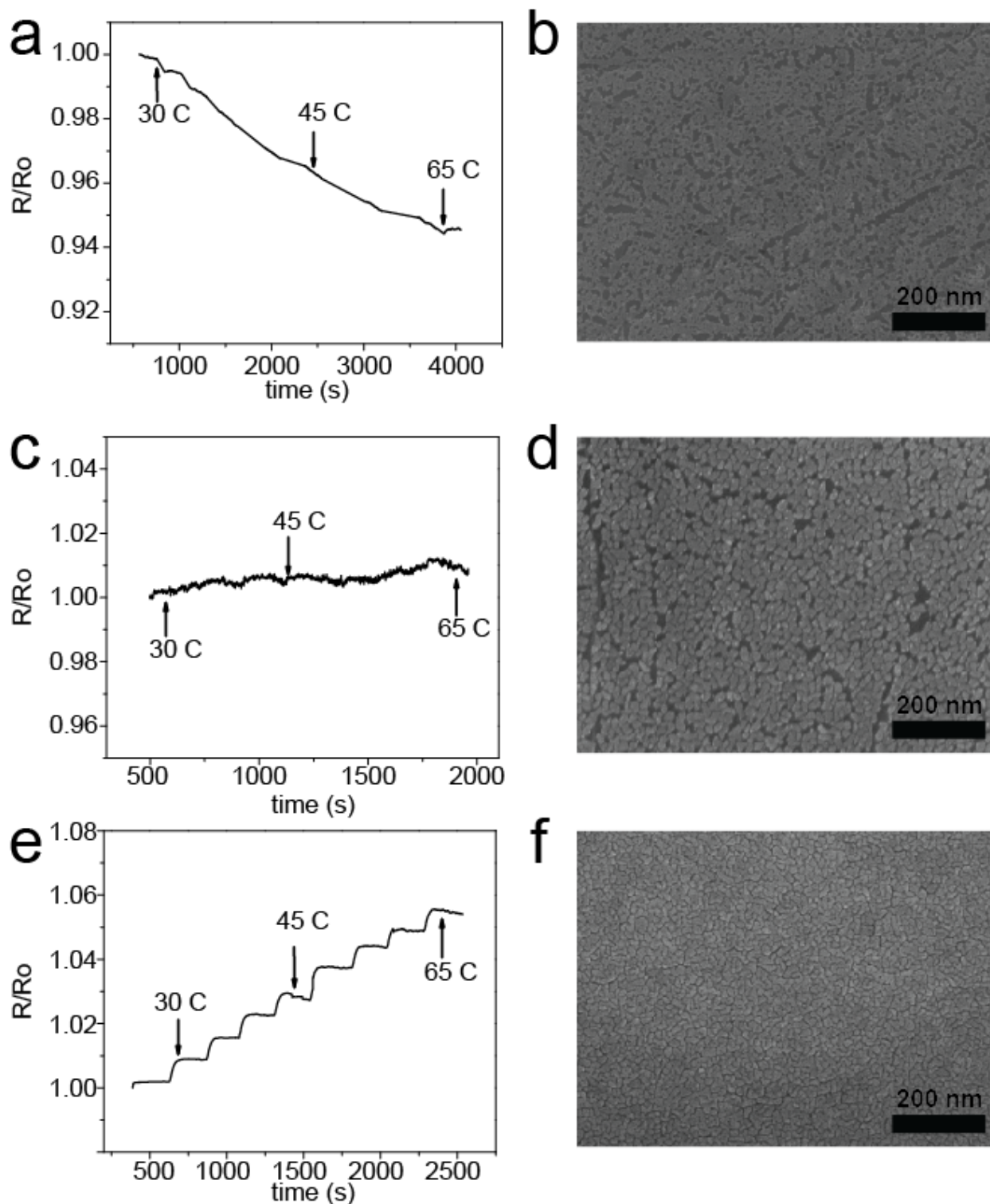


Figure S1. Thermal sensitivity and morphology of palladium nanoisland films. Normalized resistance as a function of time for palladium nanoislands of 0.5 nm (a), 0.9 nm (c), and 3 nm (e) films. The samples were heated from 30 C to 65 C over the course of the resistance measurement. SEM micrographs of 0.5 nm (b), 0.9 nm (d), and 3 nm (f) films are shown for comparison of the morphologies.

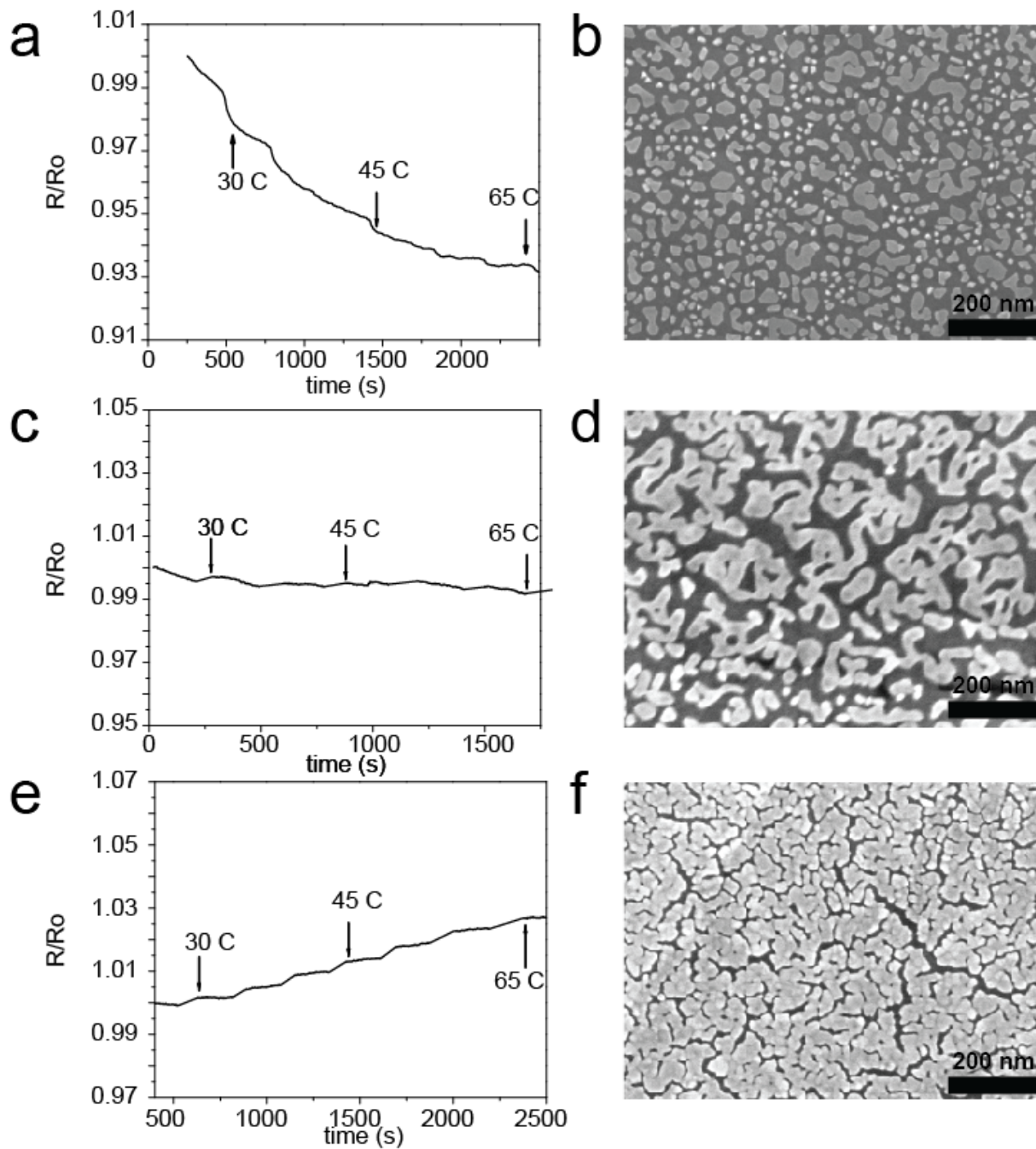


Figure S2. Thermal sensitivity and morphology of gold nanoisland films. Normalized resistance as a function of time for palladium nanoislands of 4 nm (a), 8 nm (c), and 11 nm (e) films. The samples were heated from 30 C to 65 C over the course of the resistance measurement. SEM micrographs of 4 nm (b), 8 nm (d), and 11 nm (f) films are shown for comparison of the morphologies.

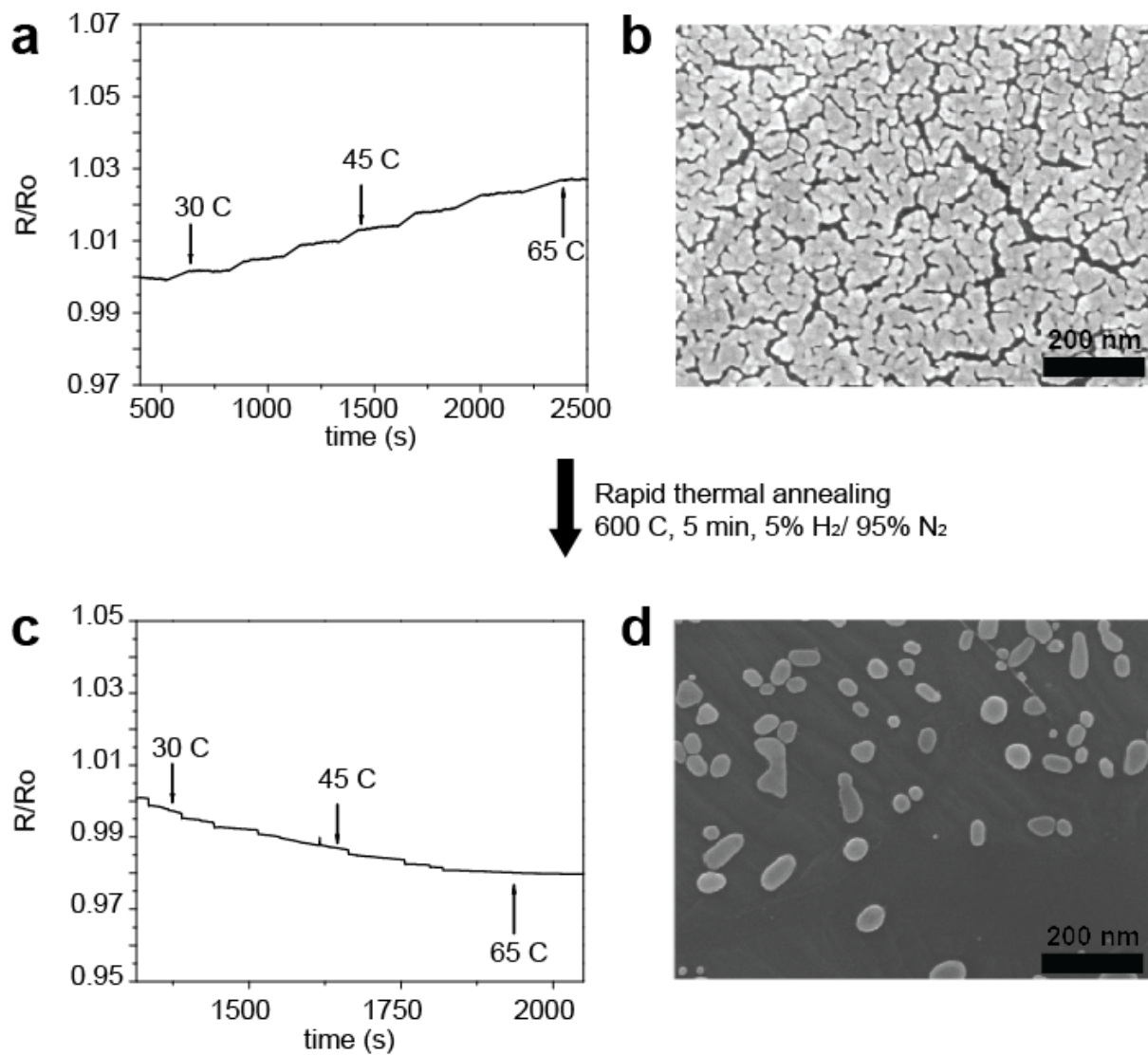


Figure S3. Effect of rapid thermal annealing on an 11 nm gold nanoisland sample. Normalized resistance as a function of time for an 11 nm gold nanoisland sample (a) and an SEM micrograph of the morphology. After rapid thermal annealing the normalized resistance as a function of time is shown (c) and the new morphology (d).

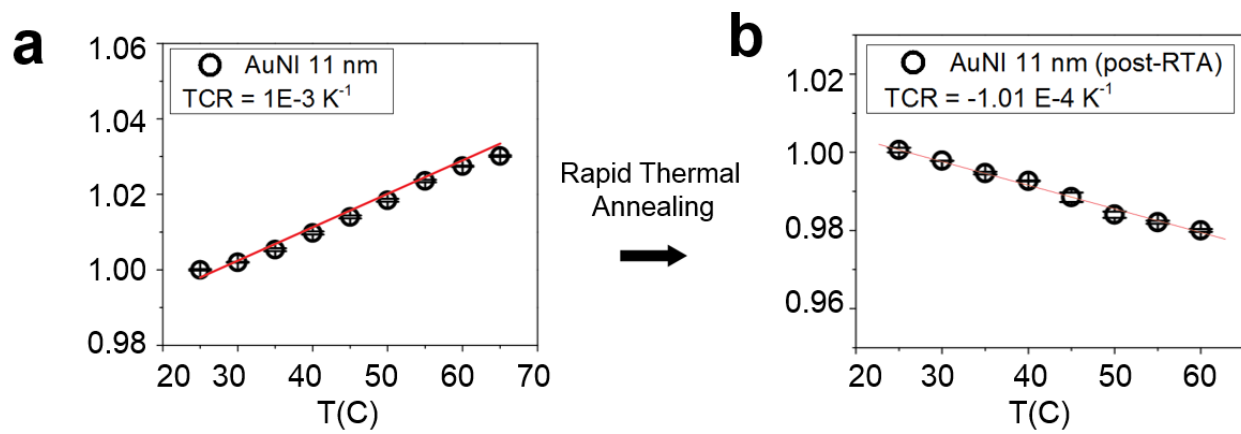


Figure S4. Effect of rapid thermal annealing on the thermal coefficient of resistance (TCR). The TCR of 11 nm gold nanoisland films is plotted before (a) and after (b) rapid thermal annealing.

Image Analysis. SEM images were analyzed using a custom python code. This code is available freely at (https://github.com/seroot/SEM_Image_Analysis). An overview of the analysis is given in Figure S5. First, an SEM image in the .tif format is imported and an SEM_IM object is instantiated. Next, the bottom of the image is cropped out, and a threshold is defined using Otsu's method, as implemented in the Mahotas python image analysis package. Finally, distinct islands are labeled separately and various properties are computed including (1) coverage (2) pixelated area of distinct islands. The quality of the image analysis is inherently limited by the resolution of the SEM image. While the algorithm works nicely for gold nanoislands, it has problems with the palladium nanoislands because of limitations on SEM resolution and contrast between the two materials.

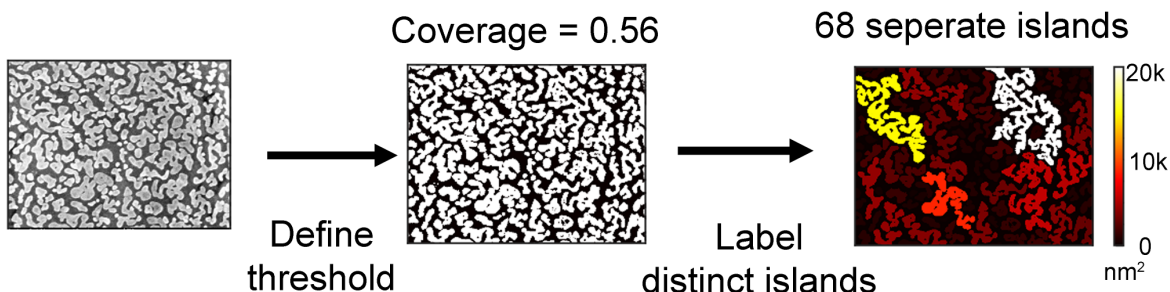


Figure S5. Image analysis of scanning electron micrographs. The flow for processing micrograph images is shown, a threshold for contrast is defined which allows nanoislands to be discerned from the underlying graphene. Average surface areas for nanoislands can then be determined.

Composite Model. A model was developed to describe the effect of surface coverage and nominal deposition thickness on the TCR of the composite material. Thin films of gold have been demonstrated to exhibit a TCR that depends on thickness. Adomov et al.² have proposed the following relation to describe this behavior:

$$\alpha_{Au} = \alpha_o \left(1 + \frac{3l}{8d} \right)^{-1}$$

Here α_{Au} is the TCR of the gold thin film, α_o is the bulk TCR of gold (3400 PPM), d is the thickness and l is the electron mean free path of gold (400 Å). This equation shows that the TCR of gold decreases with thickness following the trend shown in **Figure S6a**. The average thickness of the gold islands can be approximated as

$$d = \frac{d^*}{\theta}$$

where d^* is the nominal thickness that is measured using a quartz crystal microbalance and θ is the surface coverage computed from the image analysis.

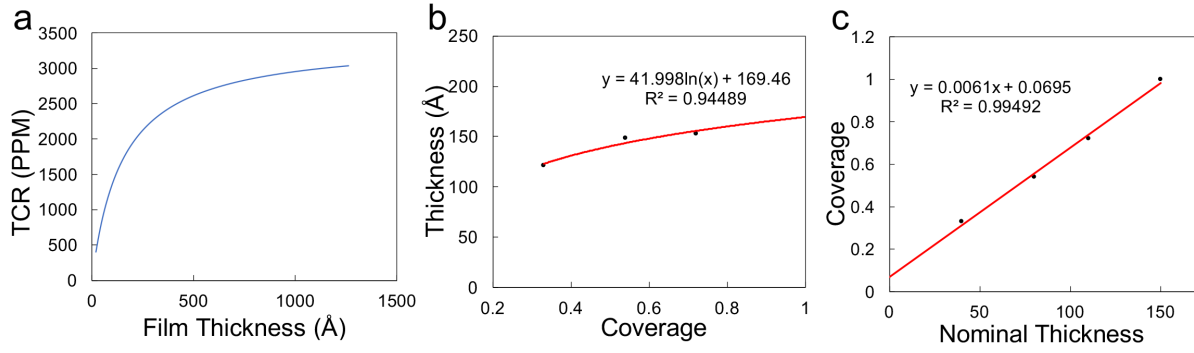


Figure S6. Theoretical models on the TCR. Adomov's model on the relation between TCR and film thickness is shown (a). (b) Coverage as a function of true film thickness. (c) The coverage is plotted as a function of nominal thickness, as measured by QCM.

As shown in **Figure S6b**, the actual thickness of the islands does not increase strongly with nominal deposition because most of the added material goes towards increasing the surface coverage, until the surface is completely covered, at which point the nominal thickness and the actual thickness should be approximately equal. Furthermore, as shown in **Figure S6c**, we observed that in the surface coverage was linearly related to the nominal deposition thickness in the island regime ($\theta < 1$).

Assuming surface coverage as the relevant fractional variable (as opposed to mass or volume fraction), we incorporated these relations into a composite theory based on the following expression:

$$\alpha_c = \theta\alpha_{Au} + (1 - \theta)\alpha_{Gr}$$

Where α_{Gr} is the TCR of graphene, which we measured to be approximately -3000 PPM. After some algebra, the following expression can be obtained:

$$\alpha_c = \alpha_{gr} - \theta \left(\frac{\alpha_o}{1 + \frac{3l\theta}{8d^*}} - \alpha_{gr} \right)$$

- (1) Coelho, L. P. Mahotas: Open Source Software for Scriptable Computer Vision. *J. Open Res. Softw.* **2013**, *1* (1), 1–13.
- (2) Adamov, M.; Perovic, B.; Nenadovic, T. Electrical and Structural Properties of Thin Gold Films Obtained by Vacuum Evaporation and Sputtering. *Thin Solid Films* **1974**, *24* (1), 89–100.

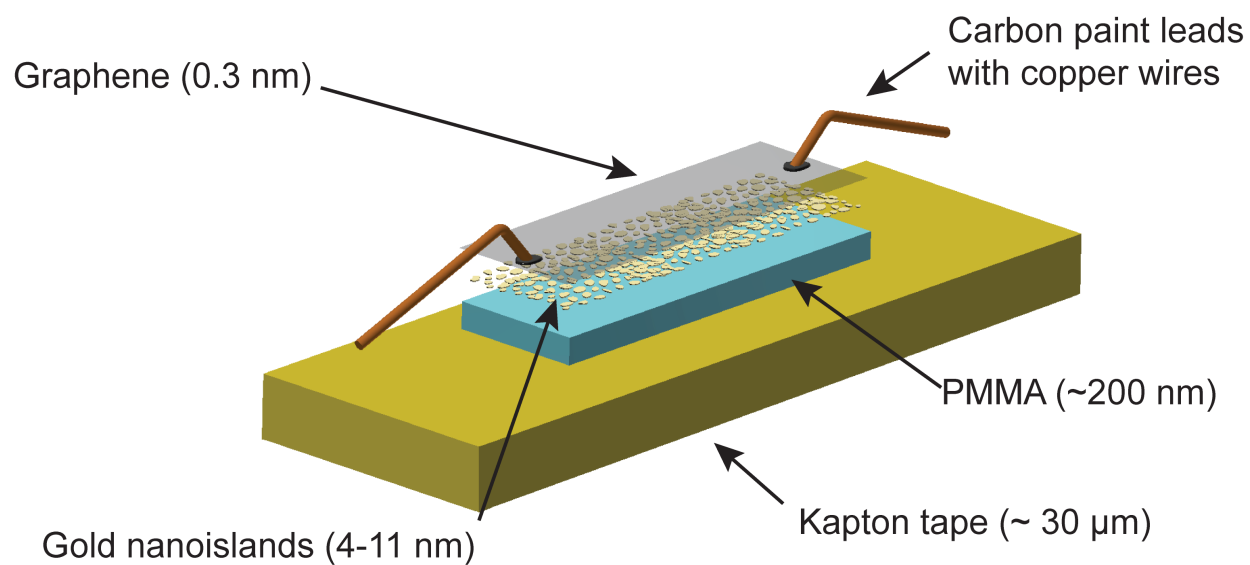


Figure S7. Schematic drawing of a near-zero TCR wearable sensor. A schematic is shown showing the order of thin film layers on a wearable sensor and their thicknesses.